

Effect of viscous dissipation on natural convection flow past an impulsively moving vertical plate with ramped temperature

Cite as: AIP Conference Proceedings **2246**, 020007 (2020); <https://doi.org/10.1063/5.0014628>
Published Online: 28 July 2020

Siva Reddy Sheri, Ch. Vijaya Bhaskar, and Anjan Kumar Suram



View Online



Export Citation

Lock-in Amplifiers
up to 600 MHz



Effect of Viscous Dissipation on Natural Convection flow Past an Impulsively Moving Vertical Plate with Ramped Temperature

Siva Reddy Sheri^{1, a)} Ch. Vijaya Bhaskar^{2, b)} and Anjan Kumar Suram^{3, c)}

¹*Department of Mathematics, GITAM University, Hyderabad Campus, Telangana, India*

²*Department of Mathematics, Vignan Institute of Technology and Science, Hyderabad, Telangana,*

³*Department of Mathematics, Christu Jyothi Institute of Technology and Science, Jangaon, Telangana, India*

^{a)}Corresponding author: sreddy7@yahoo.co.in

^{b)} vijay3284@gmail.com

^{c)}anjankumar.suram@gmail.com

Abstract. This article illustrates the influence of viscous dissipation on free convective flow past an impulsively moving vertical plate with ramped temperature. In order to analyze all the essential features, the flow governing partial differential equations are solved numerically by utilizing Finite element technique, consequently obtained results are displayed graphically. The effects of skin friction, Nusselt number and Sherwood number are exhibited in a tabular form. Comparison is made with previously published literature and a great coordination between the results exist.

Keywords: Viscous dissipation, Natural convection, Ramped temperature, FEM.

INTRODUCTION

Natural convection is often experienced in our environment and engineering devices. Free convection flow is caused by the temperature contrast and distinction in concentration of material constitution. Quite often one can see that both heat and mass transfer at a time in free convection. This investigation of flow wonders has a wide scope of utilizations in the field of science and technology for example toxic waste in water bodies, vaporization of mist and fog, photosynthesis, drying of porous solids, transpiration and sea-wind formation. Because of this one a few specialists have examined the natural convection flow, couple of commitments are Chamkha [8] explored Unsteady MHD convective heat and mass transfer past a semi-infinite vertical permeable moving plate with heat absorption. Gebhart and Pera [2] observed the steady state natural convection on a vertical plate with variable surface temperature and variable mass diffusion. Callahan and Marner [7] solved the problem of transient free convection with mass transfer on an isothermal vertical plate. Ekambavannan and Ganesan [10] discussed Finite difference analysis of unsteady natural convection flow along an inclined plate with variable surface temperature and mass diffusion. Ganesan and Palani [11] have analyzed numerically for transient free convection flow past a semi-infinite inclined plate with variable surface heat and mass flux. Seth and Khalid [9] studied hydromagnetic combined heat and mass transfer by natural convection from permeable surface embedded in a fluid-saturated porous medium

Viscous dissipation occurs in natural convection in various devices. Such dissipation effects may also be present in stronger gravitational fields and in process wherein the scale of the process is very large, e.g., on larger planets, in large masses of gas in space, and in geological processes in fluids internal to various bodies. With viscous dissipative heat included in the energy equation, Gebhart [12] studied the affect of viscous dissipation in natural convection.

Numerous authors examined for analytical or numerical solutions which are obtained by considering conditions at the plate to be constant and well defined. However many practical problems required non-uniform thermal conditions. Ahmed and Das [1] investigated Hall effect on transient mhd flow past an impulsively started vertical plate in a porous medium with ramped temperature, rotation and heat absorption Seth et al. [4] investigated numerical solution of unsteady hydromagnetic natural convection flow of heat absorbing fluid past an impulsively moving vertical plate with ramped temperature. Barik [5] discussed the chemical reaction and radiation effects of MHD free convective flow past an impulsively moving vertical plate with ramped wall temperature and concentration. Siva reddy Sheri et al.[13] have found Transient approach to heat absorption and radiative heat transfer past an impulsively moving plate with ramped temperature. Siva reddy Sheri and Anjan Kumar [14] studied Finite element analysis of heat and mass transfer past an impulsively moving vertical plate with ramped temperature. Siva reddy Sheri et al.[15] analyzed thermal-diffusion and diffusion-thermo effects on MHD natural convective flow through porous medium in a rotating system with ramped temperature. Vijay Bhaskar et al. [16] have studied MHD natural convection flow past a moving vertical plate with ramped temperature.

The present numerical investigation deals with the effect of heat and mass transfer on natural convection flow past an impulsively moving vertical plate with ramped temperature and concentration with Eckert number. The governing equations are solved using finite element method. The numerical result is validated by comparing the values of the Nusselt number, Skin friction and Sherwood number obtained through our present scheme with the earlier published results.

MATHEMATICAL FORMULATION

Assume a stream of viscous incompressible electrically conducting fluid past an infinite vertical plate embedded in a porous medium. The physical model and facilitate framework are appeared in Fig.1. Choose the Coordinate system in such a way that the x' -axis is taken along the plate in the upward way, y' -axis normal to the plane of the plate in the fluid. The physical model is illustrated in Fig 1. The liquid is pervaded by a uniform transverse magnetic field B_0 applied parallel to y' -axis. Initially at time $t' \leq 0$, both the fluid and plate are at rest with a consistent temperature T'_∞ and species concentration C'_∞ . At time $t' > 0$, the plate begins moving in x' -direction against gravitational field with time dependent velocity $U(t')$. Temperature and concentration surface of plate is raised or lowered to $T'_\infty + (T'_w - T'_\infty)t'/t_0$ and $C'_\infty + (C'_w - C'_\infty)t'/t_0$ when $t' \leq t_0$, and thereafter, for $t' > t_0$, temperature and concentration are constantly maintained at T'_w and C'_w respectively. It is assumed that there exists a homogeneous chemical reaction of first order with constant rate Kr' between the diffusing species and the fluid. Since the plate is infinite in x' and z' directions and is electrically non-conducting all physical quantities, except pressure, will be functions of y' and t' only.

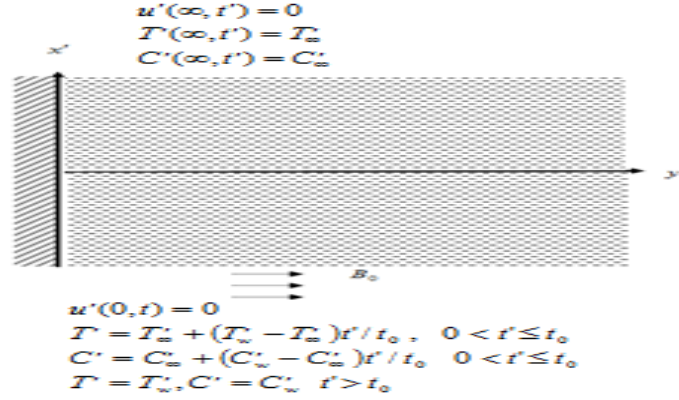


Figure 1. Physical model and coordinate system of the Problem

Taking into account the assumptions made above, the governing equations for laminar natural convection flow of a viscous incompressible electrically conducting fluid past a vertical plate in a uniform porous medium, under Boussinesq approximation, are given by

$$\frac{\partial u'}{\partial t'} = \nu \frac{\partial^2 u'}{\partial y'^2} - \frac{\sigma B_0^2}{\rho} u' - \frac{\nu}{K'} u' + g\beta'(T' - T_\infty) + g\beta^*(C' - C_\infty) \quad (1)$$

$$\frac{\partial T'}{\partial t'} = \frac{k}{\rho c_p} \frac{\partial^2 T'}{\partial y'^2} - \frac{1}{\rho c_p} \frac{\partial q'_r}{\partial y'} - \frac{Q_0}{\rho c_p} (T' - T_\infty) + \frac{\nu}{\rho c_p} \left(\frac{\partial u'}{\partial y'} \right)^2 \quad (2)$$

$$\frac{\partial C'}{\partial t'} = D \frac{\partial^2 C'}{\partial y'^2} - K'_r (C' - C_\infty) \quad (3)$$

Where u' , T' , C' , g , β' , β^* , ν , σ , ρ , k , K' , c_p , q'_r , Q_0 , D and K'_r are fluid velocity in x' -direction, temperature of the fluid, species concentration, acceleration due to gravity, volumetric coefficient of thermal expansion for species concentration, volumetric coefficient of expansion, kinematic coefficient of viscosity, electrical conductivity, fluid density, thermal conductivity, permeability of porous medium, specific heat at constant pressure, radiative flux vector, heat absorption coefficient, chemical molecular diffusivity and chemical reaction parameter respectively.

Initial and boundary conditions for the problem are specified as

$$\left. \begin{aligned} u' = 0, T' = T_\infty, C' = C_\infty \text{ for } y' \geq 0 \text{ and } t' \leq 0 \\ u' = U(t') \text{ at } y' = 0 \text{ for } t' > 0 \\ T' = T_w + (T_w' - T_w'')t'/t_0, C' = C_w + (C_w' - C_w'')t'/t_0 \text{ at } y' = 0 \text{ for } 0 < t' \leq t_0 \\ T' = T_w', C' = C_w' \text{ at } y' = 0 \text{ for } t' > t_0 \\ u' \rightarrow 0, T' \rightarrow T_\infty, C' \rightarrow C_\infty \text{ as } y' \rightarrow \infty \text{ for } t' > 0 \end{aligned} \right\} \quad (4)$$

For an optically thick fluid, Azzam [3] pointed out that in addition to emission there is also self absorption and usually the absorption co-efficient is wavelength dependent and large Bestman [6] so we can adopt the

Rosseland approximation for radiative flux vector q'_r . The radiative flux vector q'_r under Rosseland approximation becomes

$$q'_r = -\frac{4\sigma^*}{3k^*} \frac{\partial T'^4}{\partial y'} \quad (5)$$

Where k^* is mean absorption co-efficient and σ^* is Stefan-Boltzmann constant.

Assuming small temperature difference between fluid temperature T' and free stream temperature T'_∞ , T'^4 is expanded in Taylor series about a free stream temperature T'_∞ and neglecting higher order terms ($T' - T'_\infty$), we obtain

$$T'^4 \approx 4T'^3_\infty T' - 3T'^4_\infty \quad (6)$$

Making use of Equations (5) and (6) in Equation (2), we Obtain

$$\frac{\partial T'}{\partial t'} = \frac{k}{\rho c_p} \frac{\partial^2 T'}{\partial y'^2} + \frac{1}{\rho c_p} \frac{16\sigma^* T'^3_\infty}{3k^*} \frac{\partial T'^2}{\partial y'^2} - \frac{Q_0}{\rho c_p} (T' - T'_\infty) \quad (7)$$

Introducing following non-dimensional quantities and parameters

$$\left. \begin{aligned} y &= \frac{y'}{U_0 t_0}, \quad u = \frac{u'}{U_0}, \quad t = \frac{t'}{t_0}, \quad T = \frac{(T' - T'_\infty)}{(T'_w - T'_\infty)}, \quad C = \frac{(C' - C'_\infty)}{(C'_w - C'_\infty)}, \quad M = \frac{\sigma B_0^2 \nu}{\rho U_0^2}, \\ K &= \frac{K' U_0^2}{\nu^2}, \quad Gr = \frac{g\beta' \nu (T'_w - T'_\infty)}{U_0^3}, \quad Gc = \frac{g\beta^* \nu (C'_w - C'_\infty)}{U_0^3}, \quad Pr = \frac{\nu \rho c_p}{k}, \\ R &= \frac{16\sigma^* T'^3_\infty}{3kk^*}, \quad Q = \frac{\nu Q_0}{\rho c_p U_0^2}, \quad Ec = \frac{U_0^2}{c_p (T'_w - T'_\infty)}, \quad Kr = \frac{\nu Kr'}{U_0^2}, \quad Sc = \frac{\nu}{D} \end{aligned} \right\} \quad (8)$$

In view of equations (8), equations (7) and (3) reduce to the following dimensionless form:

$$\frac{\partial u}{\partial t} = \frac{\partial^2 u}{\partial y^2} + GrT + GcC - \left(M + \frac{1}{K} \right) u \quad (9)$$

$$\frac{\partial T}{\partial t} = \frac{1}{Pr} \frac{\partial^2 T}{\partial y^2} - QT - RT + Ec \left(\frac{\partial u}{\partial y} \right)^2 \quad (10)$$

$$\frac{\partial C}{\partial t} = \frac{1}{Sc} \frac{\partial^2 C}{\partial y^2} - KrC \quad (11)$$

Where $M, K, Gr, Gc, Pr, Q, R, Ec, Sc$ and Kr are magnetic parameter, permeability parameter, thermal Grashof number, solutal Grashof number, Prandtl number, heat absorption, radiation parameter, Eckert number, Schmidt number and Chemical reaction parameter respectively.

According to the above non-dimensional process the characteristic time t_0 can be defined as

$$t_0 = \frac{\nu}{U_0^2}$$

Using (8) the initial boundary conditions (4), in non-dimensional form reduces to

$$\left. \begin{aligned} u=0, \quad T=0, C=0 \quad \text{for } y \geq 0 \text{ and } t \leq 0 \\ u=1 \text{ at } y=0 \quad \text{for } t > 0, \\ T=t, C=t \text{ at } y=0 \quad \text{for } 0 < t \leq 1, \\ T=1, C=1 \text{ at } y=0 \quad \text{for } t > 1, \\ u \rightarrow 0, T \rightarrow 0, C \rightarrow 0 \quad \text{as } y \rightarrow \infty \quad \text{for } t > 0 \end{aligned} \right\} \quad (12)$$

METHOD OF SOLUTION

Numerical Solution By FEM

The non-linear dimensionless partial differential equations (9) - (11) subject to boundary conditions (12) are solved by finite element method. This method consists of following five fundamental steps: discretization of the domain, derivation of element equations, assembly of element equations, imposition of boundary conditions and solution of the system of equations. An excellent description of these steps presented in the text books by Bathe [17] and Reddy [18]. By using this procedure the whole domain is divided in to a set of 80 intervals of equal length, 0.1. At each node 3 functions are to be evaluated; hence after assembly of the elements, we obtain a set of 243 equations. The system of equations after assembly of the elements, are nonlinear and consequently an iterative scheme is employed to solve the matrix system, which is solved by using the Gauss Seidel method. This process is repeated until the desired accuracy of 10^{-6} is obtained. Hence, the finite element method is stable and convergent.

$$\text{Skin-friction coefficient } \tau \text{ at the plate is given by } \tau = \left[\frac{\partial u}{\partial y} \right]_{y=0} \quad (13)$$

$$\text{The rate of heat transfer coefficient } Nu \text{ at the plate is given by } Nu = - \left[\frac{\partial T}{\partial y} \right]_{y=0} \quad (14)$$

$$\text{The rate of mass transfer coefficient } Sh \text{ at the plate is given by } Sh = - \left[\frac{\partial C}{\partial y} \right]_{y=0} \quad (15)$$

VALIDATION OF NUMERICAL SOLUTION

To validate the numerical method employed for the solution of the present problem under some assumptions (in the absence of Eckert number) was compared with the problem of chemical reaction and radiation effects of MHD free convective flow past an impulsively moving vertical plate with ramped wall temperature and concentration by Barik [5] and are displayed in tables 1-3. These comparisons show good agreement between the results upto four decimal places. Therefore, the developed code can be used with a great confidence in the numerical results presented subsequently to study the problem considered in this paper.

Table 1. Comparison of Skin friction τ when $Ec = 0$

										Barik [5]		Present Results	
Kr	Q	t	Pr	Sc	Gc	K	Gr	M	R	Ramped	Isothermal	Ramped	Isothermal
0.2	1	0.2	0.71	2.7	0.4	0.5	2	2	4	2.0855	1.609	2.085501	1.60901
0.4	1	0.2	0.71	2.7	0.4	0.5	2	2	4	2.0859	1.6094	2.085901	1.609401
0.2	3	0.2	0.71	2.7	0.4	0.5	2	2	4	2.0926	1.6317	2.092601	1.631701
0.2	1	0.5	0.71	2.7	0.4	0.5	2	2	4	1.753	1.3535	1.75301	1.353501
0.2	1	0.2	7	2.7	0.4	0.5	2	2	4	2.1111	1.8985	2.111101	1.898501
0.2	1	0.2	0.71	0.6	0.4	0.5	2	2	4	2.083	1.6065	2.08301	1.606501
0.2	1	0.2	0.71	2.7	3	0.5	2	2	4	2.0262	1.5497	2.026201	1.549701
0.2	1	0.2	0.71	2.7	0.4	4	2	2	4	1.7391	1.147	1.739101	1.14701
0.2	1	0.2	0.71	2.7	0.4	0.5	4	2	4	2.0259	1.0729	2.025901	1.072901
0.2	1	0.2	0.71	2.7	0.4	0.5	2	4	4	1.8454	0.536	1.845401	0.53601
0.2	1	0.2	0.71	2.7	0.4	0.5	2	2	10	2.0916	1.6315	2.091601	1.631501

Table 2. Comparison of Nusselt Number (Nu) when $Ec = 0$

				Barik [5]		Present Results	
Pr	Q	t	R	Ramped	Isothermal	Ramped	Isothermal
2	1	0.2	4	1.3859	2.1297	1.385901	2.129701
0.7	1	0.2	4	0.8257	1.2689	0.825701	1.268901
2	3	0.2	4	1.2678	2.7592	1.267801	2.759201
2	1	0.5	4	2.0404	1.6499	2.040401	1.649901
2	1	0.2	10	2.1516	2.2785	2.151601	2.278501

Table 3. Comparison of Sherwood Number (Sh) when $Ec = 0$

			Barik [5]		Present Results	
Sc	Kr	t	Ramped	Isothermal	Ramped	Isothermal
2	2	0.5	1.4716	2.1005	1.471601	2.100501
2	2	0.7	1.8855	2.0467	1.885501	2.046701
4	2	0.7	2.6665	2.8944	2.666501	2.894401
4	4	0.7	2.3321	2.8356	2.332101	2.835601

RESULTS AND DISCUSSION

To investigate the effects of various parameters on flow-field in the boundary layer region, numerical values of fluid velocity, temperature and concentration are computed from the numerical solutions, are depicted graphically versus boundary layer co-ordinate y in Figs. 2–12(c) for various values of thermal Grashof number, solutal Grashof number, magnetic parameter, permeability parameter, prandtl number, thermal heat absorption coefficient, radiation parameter, Eckert number, chemical reaction parameter, Schmidt number and time. In the present study we adopted the following default parameter values of finite element computations.

$$Gr = 1.0, Gc = 1.0, M = 2.0, K = 0.2, Pr = 0.71, R = 1.0, Q = 1.0, Ec = 0.01, Sc = 2.0, Kr = 2.0 \text{ and } t = 0.5.$$

Fig. 2 displays the behavior of velocity profiles for various values of Grashof number for both ramped temperature and isothermal plates. Since thermal Grashof number Gr is the ratio of the thermal buoyancy force and viscous hydrodynamic force. From fig. 2 it is observed that velocity profile increases with the increasing of Gr in the boundary layer region. This is due the reason that the thermal buoyancy force tends to accelerate fluid flow for both ramped temperature and isothermal plates.

Fig. 3 depicts velocity profiles for various values of solutal Grashoff number for both ramped temperature and isothermal plates. Solutal Grashoff number is the ratio of the species buoyancy force and viscous hydrodynamic force. From Fig.3 it is noticed that velocity profile increases with the increasing of Solutal Grashof number Gc in boundary layer region. This due to the reason that concentration buoyancy force has a tendency to accelerate fluid velocity for both ramped temperature and isothermal plate.

Fig. 4 conveys velocity profiles for various values of magnetic field for both ramped temperature and isothermal plate. From fig. 4 it is clear that the velocity profile begins to decrease with increasing of M . The presence of magnetic field normal to the flow in an electrically conducting fluid introduces a Lorentz force which acts against the flow. This resistive force tends to slow down the flow and hence the fluid velocity decreases with increasing the magnetic field parameter

Fig. 5 explains velocity profiles for various values of permeability parameter for both ramped temperature and isothermal plate. From fig. 5 it is conformed that velocity profile increases with the increase in permeability parameter K . This is expected since when the holes of porous medium become larger, the resistive of the medium may be neglected. This implies that the resistance in porous medium which tends to accelerate flow of the fluid for both ramped temperature and isothermal plates.

Figs. 6(a) and 6(b) display the velocity and temperature profiles for different values of Prandtl number for both ramped and isothermal plates. Prandtl number is the ratio of momentum diffusivity (kinematic viscosity) to thermal diffusivity. It can be related to the thickness of the thermal and velocity boundary layers. It is actually the ratio of velocity boundary layer to thermal boundary layer. Fig 6(a) reveals that velocity profile decreases with the increasing of Pr . This implies that thermal diffusion tends to accelerate fluid velocity throughout boundary layer region. This happens due to the fact that thermal diffusion provides an impetus to the thermal buoyancy force. Fig 6(b) explains that temperature profile decreases with the increasing of Pr . Since Pr signifies the relative effects of viscosity to thermal conductivity. This implies that, thermal diffusion tends to enhance fluid temperature.

Figs. 7(a) and 7(b) demonstrate the velocity and temperature profiles for several values of heat absorption for both ramped temperature and isothermal plates. From figs 7(a) and 7(b) it is clear that fluid velocity and temperature profiles decrease with increasing of Q . This is due to the reason that, heat absorption tends to retard fluid velocity

and temperature throughout boundary layer region. This may be attributed to the fact that the tendency of heat absorption (thermal sink) is to reduce the fluid temperature which causes the strength of thermal buoyancy force to decrease resulting in a net reduction in the fluid velocity

Figs. 8(a) and 8(b) depict velocity and temperature profiles for several values of radiation parameter for both ramped temperature and isothermal plate. From these two figs it is observed that fluid velocity and temperature increase with the increasing of radiation parameter in the boundary layer region which implies that thermal radiation tends to enhance fluid velocity and temperature for both ramped temperature and isothermal plates.

Figs. 9(a) and 9(b) describe velocity and temperature profiles for several values of Eckert number on for both ramped and isothermal plate. The Eckert number is the relationship between kinetic energy in the flow and the enthalpy. It represents the change of kinetic energy into internal energy by work done against the viscous fluid stresses. From Figs 9(a) and 9(b) it is clear that there is an increase in fluid velocity and temperature due to the fact that greater viscous dissipative heat causes a rise in the velocity as well as the temperature.

Figs. 10(a) and 10(b) portray velocity and concentration profiles for different values of chemical reaction for both ramped and isothermal plates. From 10(a) and 10(b) it is observed that an increase in chemical reaction parameter leads to a decrease in both the values of velocity and concentration. This is due to fact that distinct velocity acceleration occurs near the wall after which profiles decay smoothly to the stationary value in free stream. Chemical reaction therefore boosts momentum transfer, i.e., accelerates the flow.

Fig. 11(a) and 11(b) give the details about the profiles of velocity and concentration for various values of Schmidt number for both ramped temperature and isothermal plates. From 11(a) and 11(b) it is noticed that both velocity and concentration distribution diminishes at all points of the flow field with the increase of the Schmidt number. This confirms that the heavier diffusing species have a greater retarding influence on velocity and concentration distribution of the flow field in case of both ramped temperature and isothermal plates.

Figs. 12(a), 12(b) and 12(c) display the profiles of fluid velocity, temperature and concentration for various values of time for both ramped temperature and isothermal plates. Fig 12(a) explains the effect of time on velocity. It is noticed that velocity increases on increasing time t . That is there is an enhancement in fluid velocity for both ramped temperature and isothermal plate. Fig 12(b) reveals the effect of time on temperature field for both ramped temperature and isothermal plates. It is observed that temperature enlarges on increasing time. This implies that there is enrichment in field of temperature for both ramped temperature and isothermal plates. Fig 12(c) tells the effect of time on concentration distribution. It is evident that concentration distribution increases on increasing time. This implies that, for both ramped temperature plates there is improvement in concentration with the progress of time.

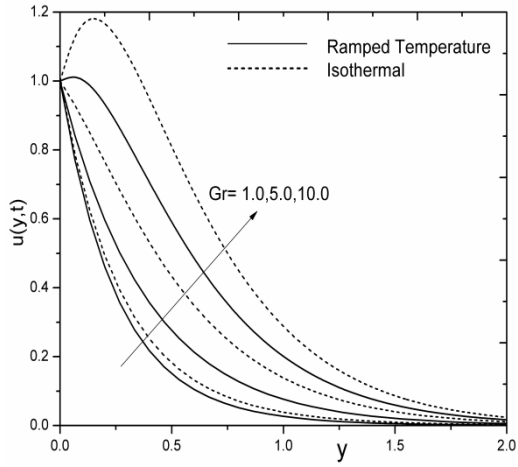


Fig. 2. Effect of Gr on velocity profile

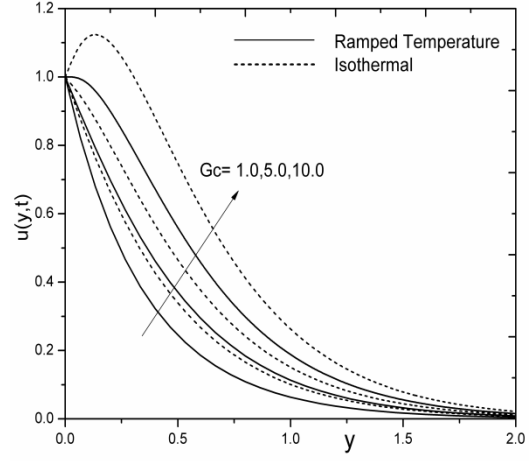


Fig. 3. Effect of Gc on velocity profile

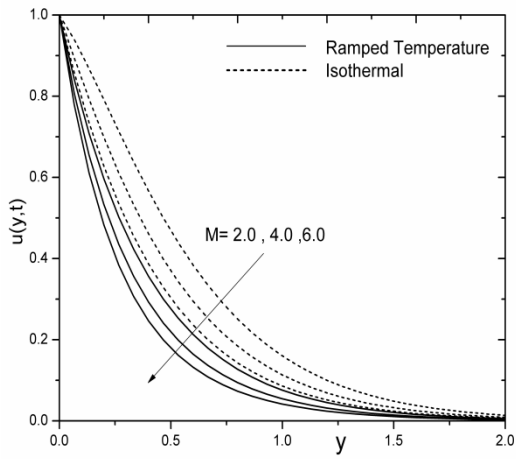


Fig. 4. Effect of M on velocity profile

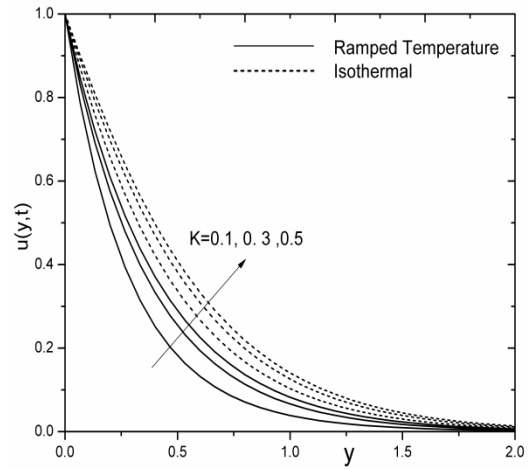


Fig. 5. Effect of K on velocity profile

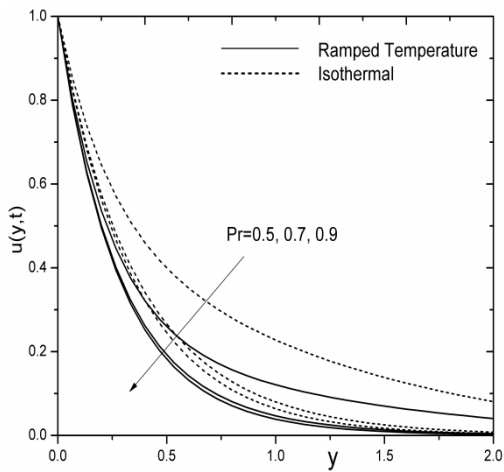


Fig. 6(a). Effect of Pr on velocity profile

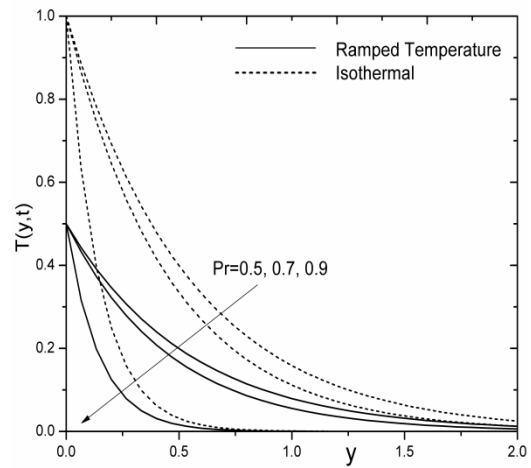


Fig. 6(b). Effect of Pr on temperature profile

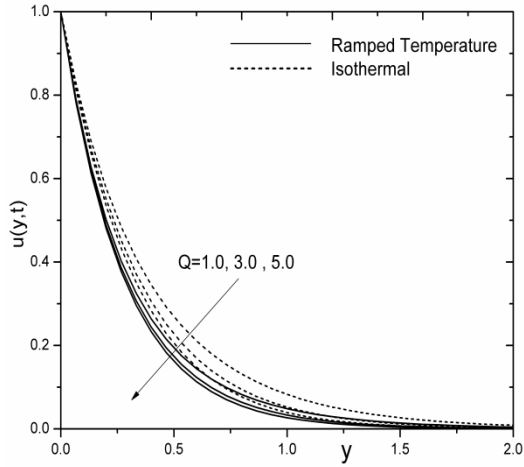


Fig. 7(a). Effect of Q on velocity profile

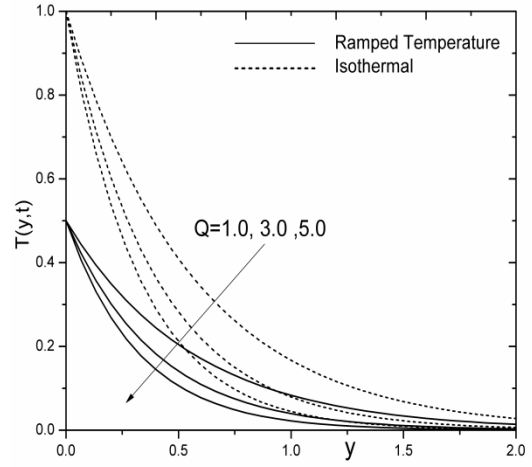


Fig. 7(b). Effect of Q on temperature profile

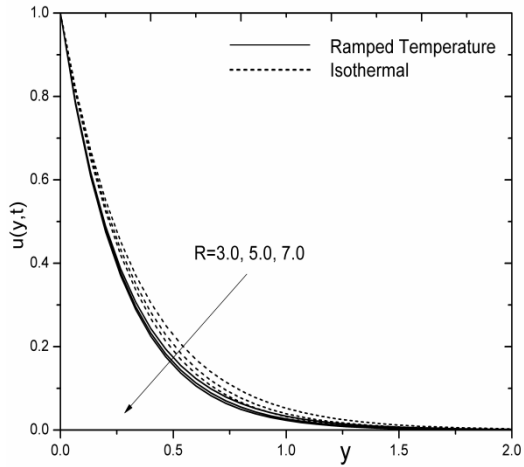


Fig. 8(a). Effect of R on velocity profile

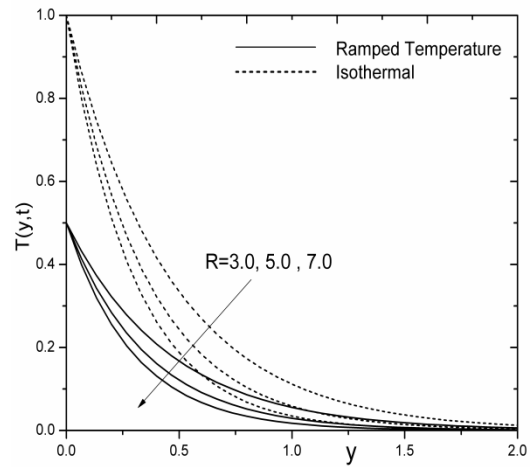


Fig. 8(b). Effect of R on temperature profile

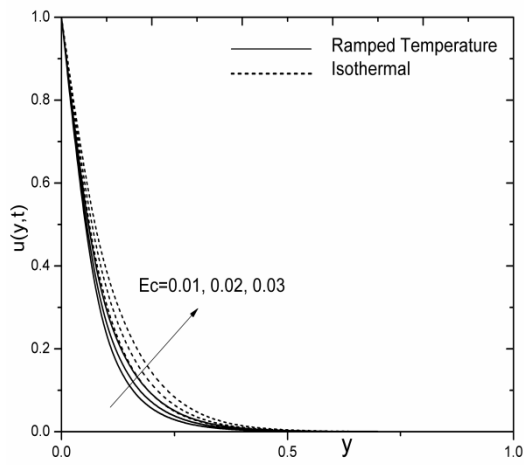


Fig. 9(a). Effect of Ec on velocity profile

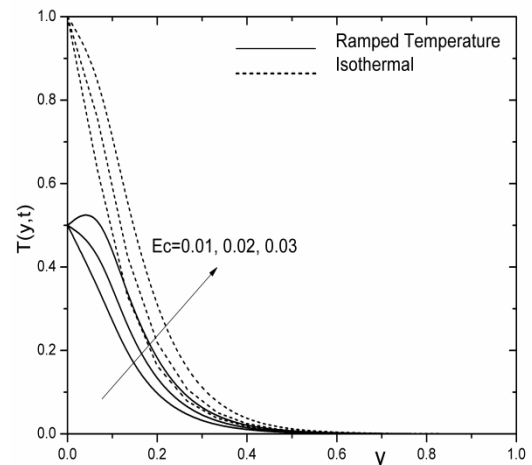


Fig. 9(b). Effect of Ec on temperature profile

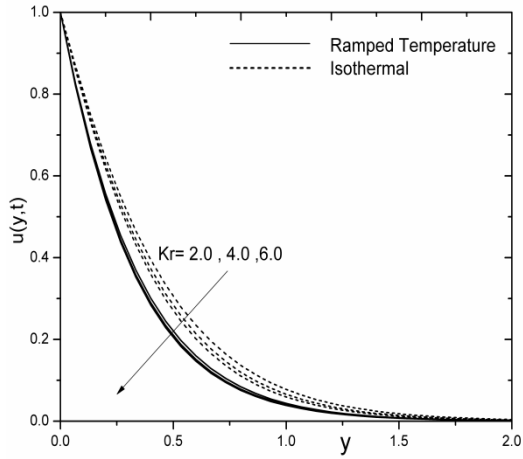


Fig. 10(a). Effect of Kr on velocity profile

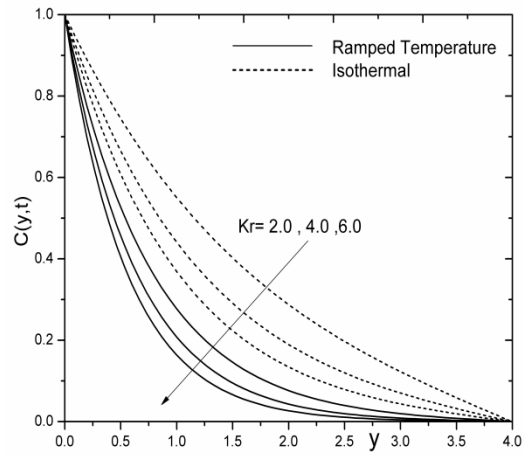


Fig. 10(b). Effect of Kr on concentration profile

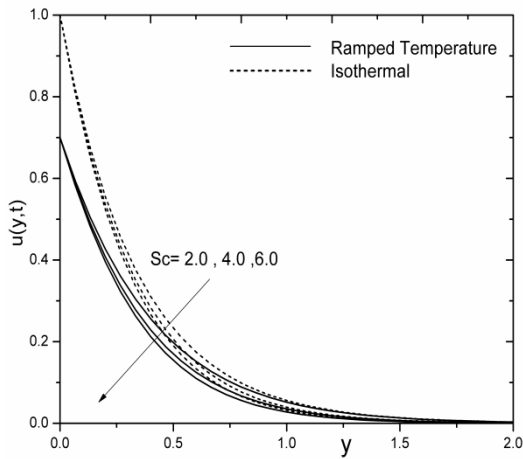


Fig. 11(a). Effect of Sc on velocity profile

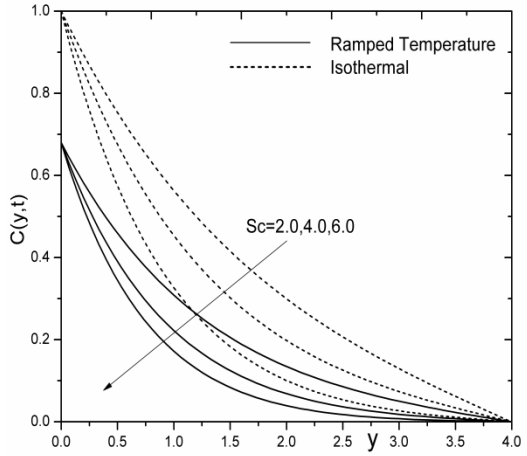


Fig. 11(b). Effect of Sc on concentration profile

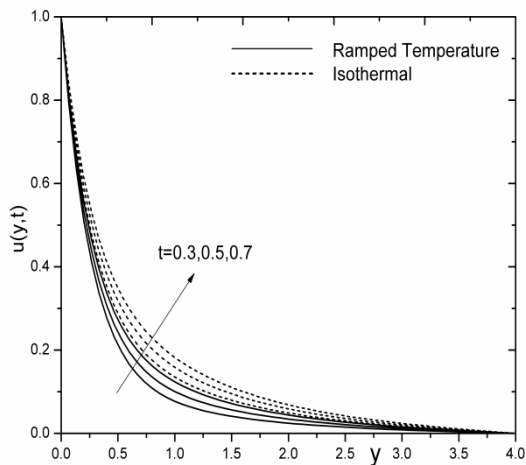


Fig. 12(a). Effect of t on velocity profile

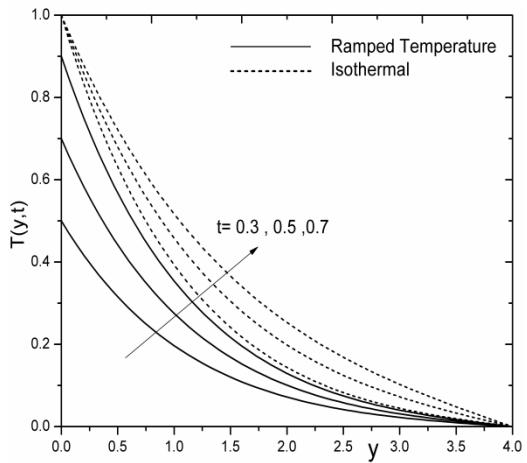


Fig. 12(b). Effect of t on temperature profile

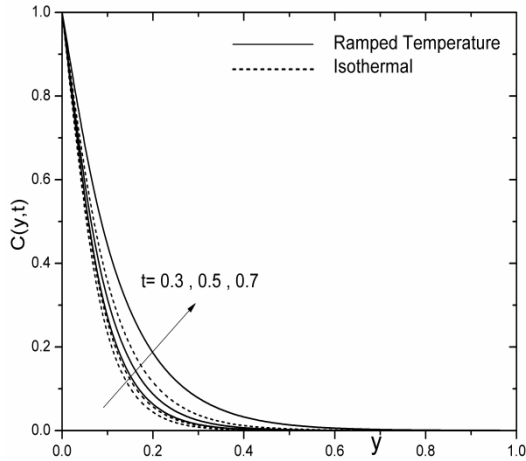


Fig. 12(c). Effect of t on concentration profile

CONCLUSIONS

The present numerical analysis deals with the effect of viscous dissipation on natural convection flow past an impulsively moving vertical plate with ramped temperature. The numerical solutions of momentum, energy and concentration equations are obtained by Finite element method. Graphical results of velocity, temperature and concentration against different flow parameters are obtained by MATLAB. Effect of Skin friction, Nusselt number and Sherwood number on flow field is presented in a tabular form and at the same time they are compared with the earlier results presented by Barik [5]. The overall conclusions for both ramped and isothermal plates are: the velocity increases with the increase of thermal buoyancy force Gr , concentration buoyancy force Gc , permeability parameter K , Eckert number Ec and time t and it has reverse tendency with the increase of magnetic parameter M , Prandtl number Pr , heat absorption Q , radiation parameter R , Chemical reaction parameter Kr and Schmidt number Sc . Temperature increases with the increase of Eckert number Ec and time t and it has reverse trend with the increase of Prandtl number Pr , heat absorption Q and radiation parameter R . Concentration increases with the increase of time t and it has reverse phenomenon with the increase of Chemical reaction parameter Kr and Schmidt number Sc .

REFERENCES

1. N. Ahmed, and K. Das, *Applied Mathematical Sciences*, **7(51)**, 2525 – 2535 (2013).
2. B. Gebhart, and L Pera, *International Journal of Heat Mass Transfer*, **14**, 2025–2050 (1971).
3. G.Azzam *Physica Scripta*, **66**, 71–76 (2002).
4. G.S. Seth, S.Sarkar, and G K.Mahato, *International journal of applied mathematical Research*, **2(2)**, 317-324(2013).
5. R. N. Barik, *European Journal of Advances in Engineering and Technology*, **1(2)**, 56-68 (2014).
6. A.R.Bestman, *International Journal for Numerical Methods in Engineering*, **21**, 899–908 (1985).
7. G. D. Callahan, and W J. Marner, *International Journal of Heat Mass Transfer*, **19**, 165–174(1976).
8. A. J. Chamkha, *International Journal of Engineering Science*, **42**, 217–230(2004).

9. A. J. Chamkha, and A. A. Khaled, *International Journal of Numerical Methods for Heat Fluid Flow*, **10(5)**, 455– 476(2000).
10. K. Ekambavannan, and P. Ganesan, *Heat and Mass Transfer*, **31** , 17–24(1995).
11. P. Ganesan, G. Palani, *Proceedings of the Fourth ISHMT/ASME Heat and Mass transfer Conference and Fifteenth National Heat and Mass Transfer Conference, Pune, India*, 323–329(2000).
12. J.B. Gebhart , *Journal of Fluid Mechanics*, **14**, 225–232(1962).
13. Siva Reddy Sheri, R.S. Raju and S.Anjan Kumar, *Procedia Engineering*,**127**,893-900(2015).
14. Siva Reddy Sheri, and S.Anjan Kumar, *Journal of Applied Science and Engineering*,**19**,385-392(2016).
15. Siva Reddy Sheri, Ali J.Chamkha, and S.Anjan Kumar, *International Journal of Numerical Methods for Heat & Fluid Flow*, **27(11)**, 2541-2480(2017).
16. Ch.Vijaya Bhaskar, Siva Reddy Sheri, and S.Anjan Kumar, *ARPJ Journal of Engineering and Applied Sciences*,**13(22)**,8846–8853(2018).
17. K J. Bathe, *Finite Element Procedures*, Prentice-Hall,New Jersey, (1996).
18. J.N. Reddy, *An Introduction to the Finite Element Method*, 3rd Edition, New York: McGraw-Hill Book Company, (2006).